J. Geomag. Geoelectr., **47**, 801–812, 1995

Radar Observations of Magnetosphere-Ionosphere Coupling at Mid and High Latitudes

John C. FOSTER

Solar-Terrestrial Environment Laboratory, Nagoya University, Japan

(Received September 6, 1994; Revised May 22, 1995; Accepted May 25, 1995)

Radar observations from Millstone Hill have identified many interesting phenomena associated with magnetosphere-ionosphere coupling processes at the equatorward edge of the auroral region. A number of important magnetospheric boundaries are found near the latitude of the radar facility (55° magnetic) and these result in the structure and dynamics which characterize the pre-midnight sub-auroral ionosphere. The equatorward extent of the plasma sheet particle population lies on field lines near the plasmapause and precipitation from the plasma sheet alters the ionospheric conductances, currents and fields. During disturbed conditions, an intense (>100 mV/m) polarization electric field can be set up when freshly-injected plasma sheet ions lie equatorward of the electrons and this drives the latitudinally-narrow polarization jet or Sub-Auroral Ion Drifts (SAID) which directly or indirectly result in a variety of ionospheric phenomena in the pre-midnight sector. Associated with the region of strongest convection, a deep, narrow *F* region trough forms while, equatorward of this, sunward advection of plasma from later local times and lower latitudes leads to the region of Storm-Enhanced Density (SED). The pre-midnight polarization jet produces strong frictional heating near the *F* peak resulting in an expansion of the topside and heavy ion outflow which populates the magnetosphere with ionospheric O^+. Stable Auroral Red arcs (SAR arcs) occur within the narrow trough, coincident with the polarization jet electric fields and the elevated electron temperatures found there.

1. Instrumentation

The Millstone Hill Observatory is located in eastern Massachusetts at 42.6°N latitude, 288.5°E longitude (55°Λ) and is well situated to observe effects related to magnetosphere-ionosphere coupling near the plasmapause, the inner edge of the ring current, and the ionospheric trough. The Millstone Hill UHF incoherent scatter radar has been in operation through several solar cycles and is used to monitor ionospheric features and response over the altitude range 100 km to 1000 km with a typical altitude/spatial resolution of 50 km. The radar operates at 440 MHz (68-cm wavelength) with a 2.5 MW peak power and a 6% duty cycle. Its fully-steerable 46-m antenna provides wide-ranging spatial coverage, spanning >30° of latitude and 4+ hours of local time at *F* region heights. The equatorward offset of the north geomagnetic pole nearly along the Millstone Hill meridian brings high-latitude and auroral phenomena into the Observatory's near field of view during disturbed conditions and particularly during magnetic storms.

2. Mid-Latitude Coupling Phenomena

As the level of geomagnetic disturbance increases, the electric fields and particle populations which characterize the auroral region expand equatorward and their effects are felt at previously sub-auroral latitudes. A number of important magnetospheric boundaries are found near the auroral/sub-auroral transition (nominally near 60° magnetic) and these result in the ionospheric structure and dynamics which characterize the local ionospheric observations made from Millstone Hill. The high-altitude plasmapause maps down to the region near the equatorward edge of the (mid-latitude) ionospheric trough and is associated with the boundary between the corotating inner magnetosphere and the strong convection electric fields which drive the ionospheric circulation at auroral latitudes. These often-intense electric

fields serve to deepen the trough and redistribute the ionospheric plasma through advection from one local time region to another. The equatorward extent of the plasma sheet particle population lies on field lines near the plasmapause and precipitation from the plasma sheet alters the ionospheric conductances, currents and fields. During disturbed conditions, an intense (>100 mV/m) polarization electric field can be set up when freshly-injected plasma sheet ions lie equatorward of the electrons (Galperin *et al.*, 1974) and this drives the latitudinally-narrow polarization jet or Sub-Auroral Ion Drifts (SAID) (Spiro *et al.*, 1979) which directly or indirectly are responsible for a variety of ionospheric phenomena in the premidnight sector. Associated with the region of strongest convection, a deep, narrow *F* region trough forms (Schunk *et al.*, 1976) while, equatorward of this, sunward advection of plasma from later local times and lower latitudes leads to the region of Storm-Enhanced Density (SED) (Foster, 1993). This plasma is rapidly transported to and through the cusp at noon where it becomes a source of the *F* region patches which populate the polar cap ionosphere (Buchau *et al.*, 1985). The pre-midnight polarization jet produces strong frictional heating near the *F* peak, as the ions are driven through the background neutral atmosphere and this results in heavy ion outflow which populates the magnetosphere with ionospheric O^+ (Yeh and Foster, 1990). Stable Auroral Red arcs (SAR arcs) occur within the narrow trough, coincident with the polarization jet electric fields and the intensity of their 630.0 nm emission can be explained in terms of the elevated electron temperatures found there (Foster *et al.*, 1994). The variety of phenomena observed regularly from Millstone Hill is associated with the magnetosphere-ionosphere coupling processes occurring at the equatorward limit of the auroral region. Such processes often result in the growth of ion-acoustic turbulence which leads to enhanced radar backscatter (ERB) which provides a diagnostic of the associated coupling phenomena (Foster *et al.*, 1988).

2.1 Electric field equatorward extent and structure

Sunward convection spans most of the auroral region in the pre-midnight sector and usually the convection speed reaches a maximum just equatorward of the sunward/anti-sunward reversal and then decreases with decreasing latitude away from this point. Under disturbed geomagnetic conditions, the latitudinal profile of the westward ion convection (equivalent to a poleward-directed electric field) observed by the Millstone Hill radar at dusk, often exhibits a double peak (dual maxima) (Yeh *et al.*, 1991). The separation of these regions increases with increasing disturbance level, the intensity of the sunward convection in the two regions is not well correlated, and the more equatorward region of westward plasma drift can persist well after local midnight when the higher-latitude convection has reversed direction. Simultaneous overflights of the DMSP satellite reveal that the high-latitude ion drift peak coincides with the boundary plasma sheet/central plasma sheet transition and lies in the high ionospheric conductivity region while the low-latitude ion drift peak lies between the equatorward edges of the electron and soft (<1 keV) ion precipitation in a region of low ionospheric conductivity (<1 mho). The low-latitude drift peak is also associated with the latitude of maximum O^+-dominated ring current energy density.

Figure 1 (from Yeh *et al.* (1991)) presents typical latitudinal profiles of east-west ion convection velocity observed with the Millstone Hill incoherent scatter radar in the evening MLT sector for three levels of the activity index, *Kp*. The convection pattern shifts equatorward and expands as *Kp* increases and pronounced dual maxima form as *Kp* reaches more disturbed levels (*Kp* > 4). In Fig. 2 (from Yeh *et al.* (1991)) the storm-time convection profile of Fig. 1 (lower panel) is compared with simultaneous particle observations which indicate the relationship of the ionospheric convection to the overlying magnetospheric regions. The DMSP ion energy density <30 keV indicates the extent of the plasma sheet population, and the AMPTE energetic ion profile indicates that the lower-latitude drift maximum coincides with the energetic ring current in the region of low precipitation-produced ionospheric conductance (middle panel).

Electric field shielding in the equatorial magnetosphere arises when the inward transport of injected plasma in the time varying magnetic and convection electric fields, combined with the corotation electric field, results in electron and ion separation and the formation of plasma pressure gradients. In the theoretical treatment of Southwood and Wolf (1978), a northward electric field and rapid sunward

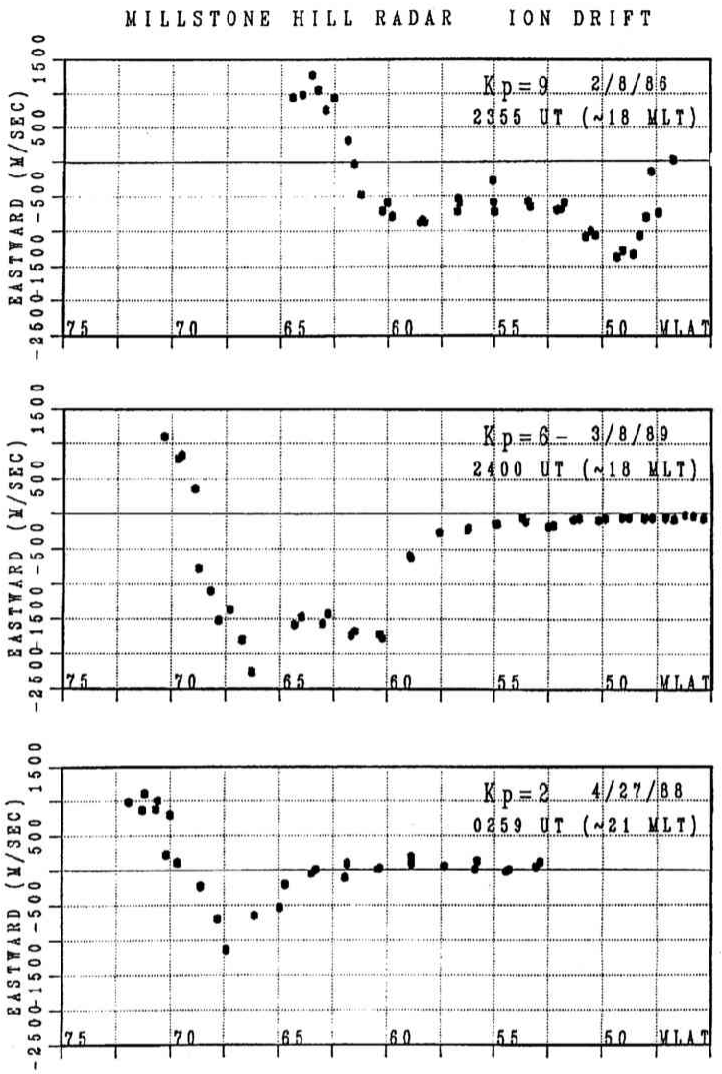

Fig. 1. Latitudinal profiles of east-west ion convection velocity observed with the Millstone Hill incoherent scatter radar in the evening MLT sector for three levels of the activity index, *Kp* (from Yeh *et al.* (1991)). The convection pattern shifts equatorward and expands as *Kp* increases and pronounced dual maxima form as *Kp* reaches moderately disturbed levels ($Kp > 4$).

convection at subauroral latitudes are created when a disturbance results in the penetration of partial ring current ions to a lower L shell than the plasma sheet electrons. The strength of this electric field is inversely related to the latitudinal separation of the particle boundaries. These effects couple to the ionosphere by particle precipitation, ionospheric conductivity, and field-aligned currents to control the convection structure and to prevent the convection electric field from further inward penetration. The low-latitude drift peak is the ionospheric signature of the electric field shielding effect associated with ring current penetration into the outer layer of the plasmasphere. A polarization (charge-separation) electric field is set up across this region and this results in the lower-latitude ion drift feature observed by the radar. The persistence of this feature at ionospheric heights, observed by the radar, is related to the long-term nature of this reconfiguration of the magnetospheric particle populations during disturbed conditions.

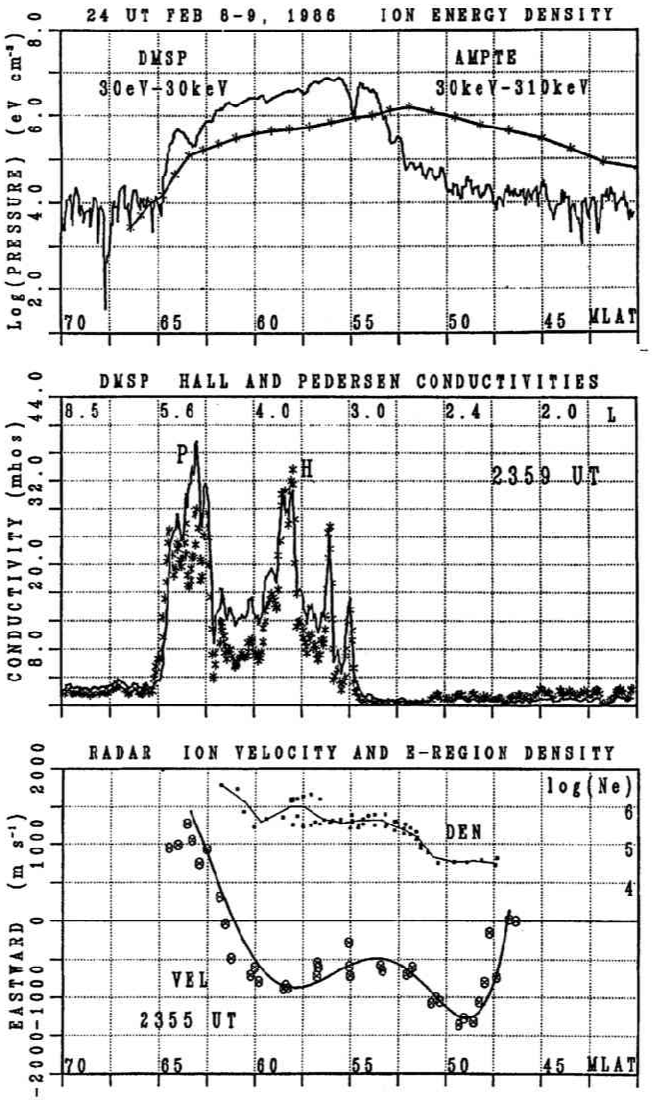

Fig. 2. Storm-time convection profile of Fig. 1 (lower panel) is compared with simultaneous particle observations which indicate the relationship of the ionospheric convection to the overlying magnetospheric regions (from Yeh *et al.* (1991)). The DMSP ion energy density <30 keV (top panel) indicates the extent of the plasma sheet population, and the AMPTE energetic ion profile indicates that the lower-latitude drift maximum coincides with the energetic ring current in the region of low precipitation-produced ionospheric conductance (middle panel).

2.2 Frictional heating and heavy ion outflow

The intense sunward plasma convection driven by magnetospheric electric fields produces strong ion-neutral frictional heating when the relative velocity between the ions and neutrals exceeds 1000 m s^{-1}. Figure 3 (from Yeh and Foster. (1990)) presents a scatter plot of ion temperature and ion convection velocity from the vicinity of a strong east/west-extended convection channel observed with the Millstone Hill radar. The observed ion temperature increase with velocity is that expected due to collisional (frictional) heating due to ion-neutral collisions (the solid curve is the empirical frictional heating relationship derived by St.-Maurice and Hanson (1982) for an exospheric temperature of 1800°K).

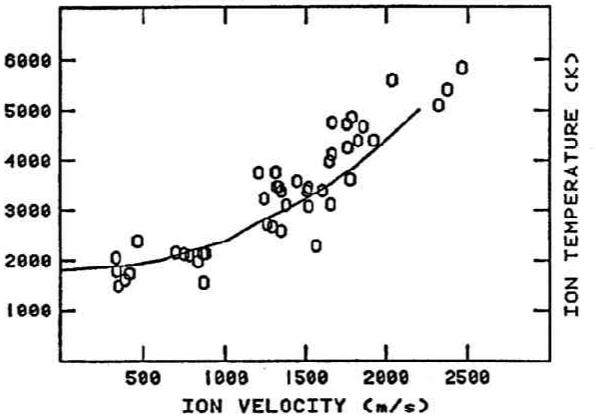

Fig. 3. Scatter plot of ion temperature and ion convection velocity from the vicinity of a strong east/west-extended convection channel observed with the Millstone Hill radar (from Yeh and Foster. (1990)). The observed ion temperature increase with velocity is that expected due to collisional (frictional) heating due to ion-neutral collisions.

Frictional heating can elevate the ion temperature to above 4000°K near the *F* peak altitude and this results in strong heavy ion outflow from the topside *F* region. Figure 4 presents altitude profiles of ionospheric parameters observed looking vertically into the heated region above Millstone Hill (42.5°N geographic latitude; 55°Λ). The observed incoherent scatter spectra (not shown) indicate that O^+ is dominant ion species below 1000 km altitude. Ion outflow speeds approach 3000 m s^{-1} at 1000 km altitude and upward-directed O^+ fluxes of 3×10^9 $cm^{-2}s^{-1}$ were observed. The analysis of the event presented by Yeh and Foster (1990) indicates that ions can be accelerated to near-supersonic outflow speeds by a time-dependent diffusion process triggered by a sudden change in heating rate near the peak altitude. The resultant mid-latitude outflow of O^+ is a significant source for heavy ions at magnetospheric heights during storm-time conditions.

2.3 Sunward plasma transport

Associated with the large-scale enhancement of the ionospheric convection electric field during disturbed geomagnetic conditions, solar-produced *F* region plasma is transported to and through the noontime cleft from a source region at middle and lower latitudes in the afternoon sector. This phenomenon has been identified in the wide-latitude coverage experiments at Millstone Hill and the characteristics of storm-enhanced density (SED) have been discussed by Foster (1993). Elevation scans in the north-south meridional plane have been used to prepare event maps which detail the temporal evolution of the electron density at 500 km altitude over a 35° span of latitude. Data which illustrate the radar observations during disturbed, greatly disturbed, and quite activity conditions (as determined by the daily *Kp*) are presented in Fig. 5, centered on O UT (19 MLT along the Millstone meridian). Sunrise occurs near 14 UT and the ionospheric trough appears at higher latitudes after 18 UT each day. For disturbed conditions, the trough is seen at lower latitudes and earlier local times, well into the sunlit *F* region. Of particular interest is the appearance of a latitudinally narrow region of enhanced density equatorward of the trough in the postnoon sector which descends in latitude as the evening progresses. The latitude of this feature is found to correspond to the equatorward extent of sunward (westward) plasma convection as the storm-enhanced density is convected towards noon from lower latitudes and later local times. The source of this plasma is solar production in the mid- and low-latitude ionosphere and strong convection near the equatorward extent of the afternoon convection cell carries this higher-density plasma toward noon and into the polar cap.

Individual azimuth and elevation scans reveal the latitude/longitude or latitude/altitude extent of the

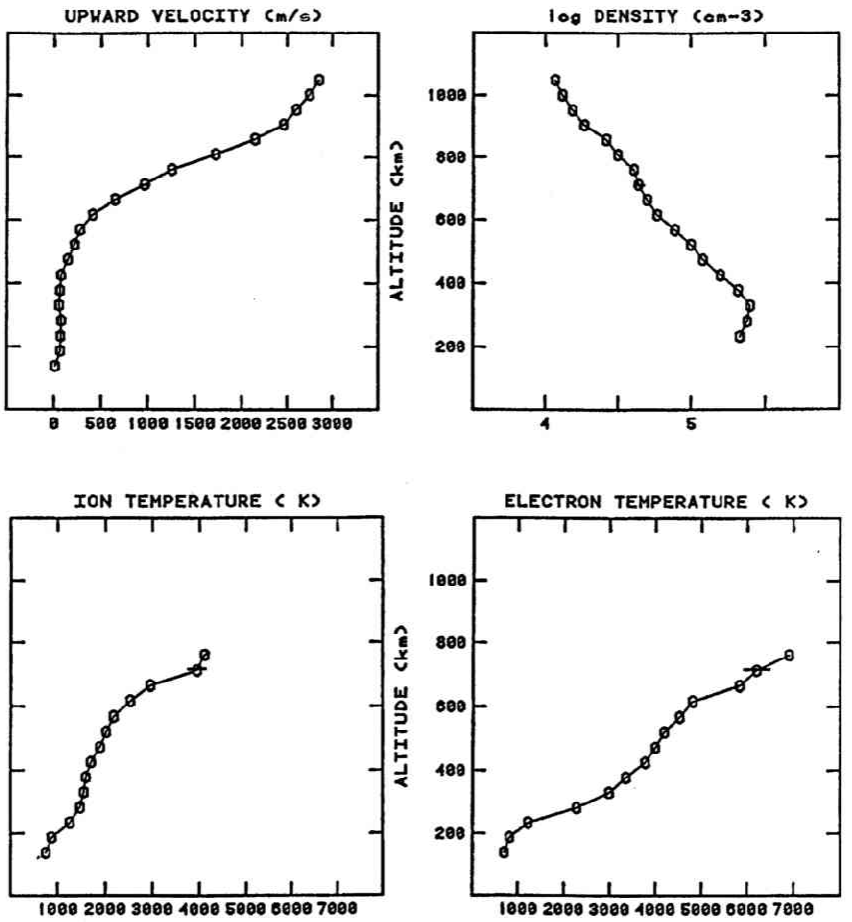

Fig. 4. Altitude profiles of ionospheric parameters observed looking vertically into a region of strong frictional heating above Millstone Hill. Ion outflow speeds approach 3000 m s^{-1} at 1000 km altitude and upward-directed O^+ fluxes of 3×10^9 $cm^{-2}s^{-1}$ were observed (from Yeh and Foster, 1990).

SED. Figure 6 presents azimuth scan data looking poleward from Millstone Hill which cover 5 hours of local time (centered near 10 MLT) and 20° of latitude. Convection is from east to west across the poleward half of the scan and enters polar cap latitudes at the farthest ranges to the NW of the radar. Enhanced density is seen to follow the convection from the region of solar production at the lower right and is swept into the polar cap across the cusp. The lower portion of the figure presents an elevation scan through this region showing the sunward-convecting region of SED as a distinct high-altitude enhanced-density region poleward of 58° latitude. This feature is often observed from Millstone Hill in the pre-midnight sector. For a given local time, SED occurs at a lower latitude for increasing levels of disturbance. During strong disturbances, the topside SED is observed to be convecting sunward at 750 m s^{-1} with a flux of 10^{14} $m^{-2}s^{-1}$. The characteristics of SED depend on the geographic longitude of the observation since the offset between the geographic and geomagnetic poles plays an important role in SED formation.

As a result of the offset between the geographic and geomagnetic poles, the afternoon sector region of sunward convection shifts to increasingly lower geographic latitude throughout the interval between 12 UT and 20 UT. A snowplow effect occurs in which the convection cell continually encounters fresh corotating ionospheric plasma along its equatorward edge, producing the latitudinally-narrow region of storm-enhanced plasma density which is advected towards higher latitudes in the noon sector. After

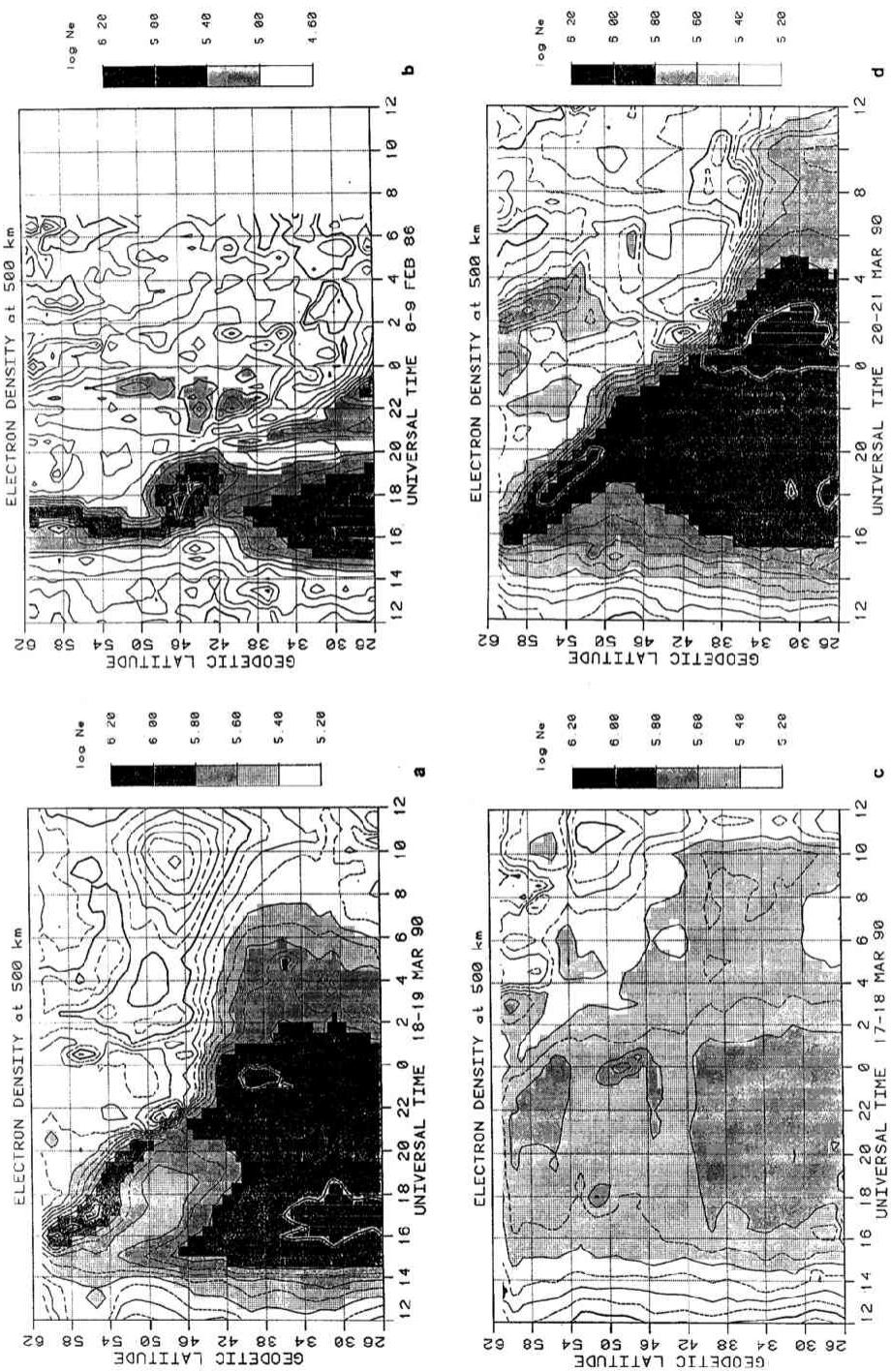

Fig. 5. Radar observations of F region density during disturbed ((a) and (d)), greatly disturbed (b), and quiet (c) activity conditions show that the ionospheric trough appears at higher latitudes after 18 UT each day (from Foster, 1993). For disturbed conditions, the trough is seen at lower latitudes and earlier local times, well into the sunlit F region. Of particular interest is the appearance of a latitudinally narrow region of enhanced density equatorward of the trough in the postnoon sector which descends in latitude as the evening progresses.

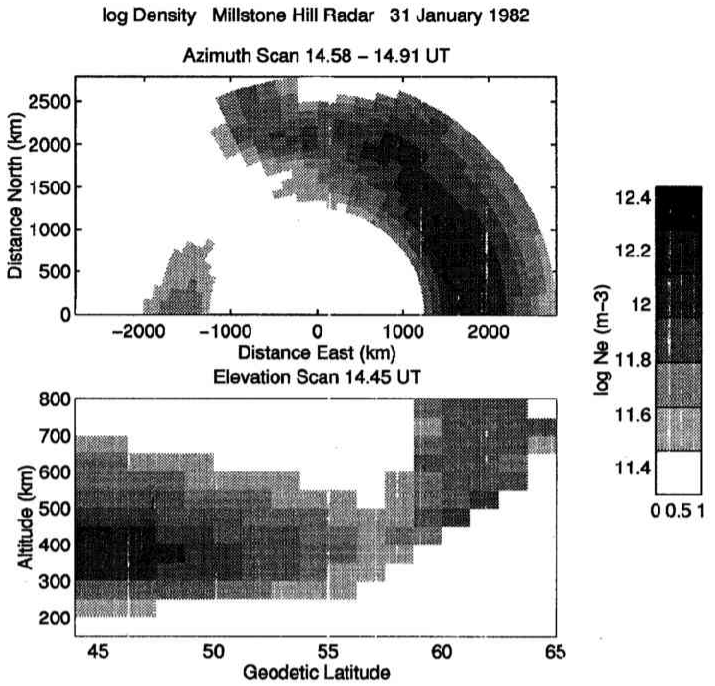

Fig. 6. Azimuth scan data looking poleward from Millstone Hill covering 5 hours of local time (centered near 10 MLT) and 20° of latitude. Convection is from east to west across the poleward half of the scan and enters polar cap latitudes at the farthest ranges to the NW of the radar. Enhanced density is seen to follow the convection from the region of solar production at the lower right and is swept into the polar cap across the cusp. The lower portion of the figure presents an elevation scan through this region showing the sunward-convecting region of SED as a distinct high-altitude enhanced-density region poleward of 58° latitude.

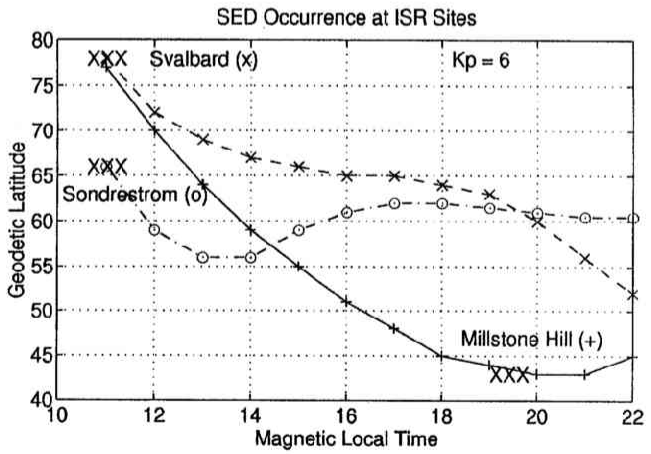

Fig. 7. Three curves depict the configuration of the region of Storm-Enhanced Density (equatorward extent of the afternoon sunward convection cell presented in geodetic latitude-MLT coordinates) at the Universal Times when three high-latitude incoherent scatter radars encounter the SED plasma. The radars at Svalbard (09 UT) and Sondrestrom (14 UT) encounter the SED region near noon local time, but at a UT when the convection pattern does not extend to appreciably lower geographic latitude. Millstone Hill, however, encounters the SED near the time of maximum latitude penetration (19 UT) when the convection pattern rapidly transports pre-midnight plasma towards noon.

24 UT, the equatorward motion of the convection boundary in geographic coordinates is reversed, the source of fresh plasma ends, and the SED fades in intensity. The instantaneous position of the longitudinally extended region of SED is determined by the equatorward edge of the convection electric field, which presents a smooth contour in geomagnetic coordinates. The extent of this boundary in geographic latitude and local time changes with Universal Time and differs considerably at the time the individual incoherent scatter radar sites encounter this feature. Figure 7 is based on the observations of SED presented by Foster (1993) and indicates that radars at Svalbard and Sondrestrom encounter the SED region near noon, but at a UT when the convection pattern does not extend to appreciably lower geographic latitudes. Millstone Hill, however, encounters the SED near the time of maximum latitude penetration when the convection pattern rapidly transports pre-midnight plasma towards noon. The SED phenomenon is expected to be seen at Svalbard and Sondrestrom, but it will not be as pronounced as when seen from the Millstone meridian.

2.4 SAR arc

During a disturbed interval in March 1990, the characteristics of a SAR arc were observed continuously from the Millstone Hill Observatory through an 8-hour interval from dusk till after midnight. The arc was co-located with a deep, narrow plasma trough and a region of enhanced westward plasma convection of similar width situated immediately equatorward of the low-latitude extent of plasma sheet particle precipitation. The associated region of westward (sunward) convection had many of the characteristics of the SAID (Sub-Auroral Ion Drifts) phenomenon and was clearly separate from the usual, more-poleward, region of auroral sunward convection, similar to events reported in the study by Yeh *et al.* (1991) and referred to as the more-equatorward ion drift maximum in the section above.

Incoherent scatter radar elevation scans revealed the latitude/altitude structure of the ionospheric features associated with this SAR arc. Figure 8 presents radar observations of the ionospheric trough 8(a) and electron temperature enhancement 8(b) which accompanied the arc, as observed along the Millstone Hill meridian at the time of a DMSP satellite overflight. The latitude profile of the red-line intensity observed with the Millstone Hill Observatory all-sky imager (Mendillo *et al.*, 1989), is shown in Fig. 8(d) to indicate the alignment of the temperature and density features with the SAR arc. The radar-scan data show a density trough at all heights at the latitude of the arc and a corresponding increase in electron temperature to >2500°K at the *F* region peak height near 480 km. Panel 8(c) superimposes the ionospheric convection velocity measurements (in the corotating frame) made with the DMSP drift meter (solid line) and with the Millstone Hill radar (discrete points) during an azimuth scan to the west of the satellite meridian. The magnitude and spatial breadth of the sunward convection region associated with the trough and SAR arc are nearly identical in the satellite and radar observations, as is the separation from a second sunward convection region associated with auroral-latitude phenomena at higher latitude (50°). The close relationship between the location of the SAR arc, the trough, and the isolated, more equatorward, region of westward convection, as seen in Fig. 8, persisted for the course of the event.

Figure 9 presents a composite picture of the magnetospheric and ionospheric features associated with this SAR arc. In panel 9(a) are presented in situ density measurements from the DMSP F9 satellite, during its overflight along the –75° meridian, which showed a >5× decrease in a 2°-wide trough co-located with the arc. The digital 630.0 nm image has been sampled along the –75° meridian at the time of the satellite overflight and these data are presented in panel 9(b). The red-line emission had a maximum intensity of 210 R above background, was sharply peaked at 43.5° and spanned 2° of geodetic latitude. An increase to the instrument saturation level (>400 R) was associated with the bright aurora to the north. High-resolution ion drift meter data, presented in panel 9(d), show upward velocities of 50 m s^{-1} immediately equatorward of the arc and downward drift of the same magnitude associated with the arc itself. The horizontal (E-W) drift was dramatic, with the SAR arc and density trough situated within a 3°-wide region of westward (sunward) convection with a maximum velocity of 550 m s^{-1} (in the inertial reference frame, corrected for co-rotation) on the immediate equatorward edge of the arc. Sunward convection was associated with the arc throughout the event.

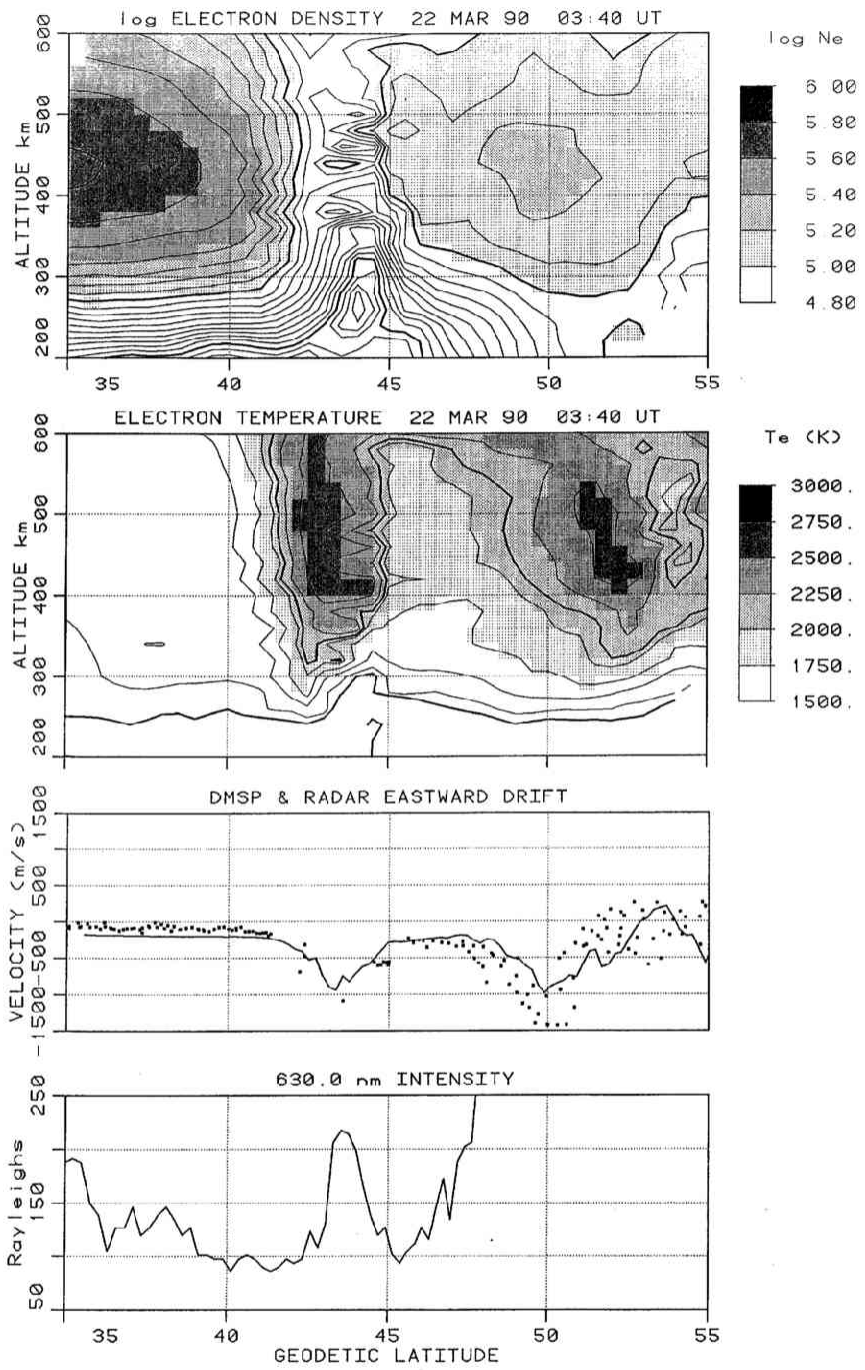

Fig. 8. Radar observations of the ionospheric trough (a) and electron temperature enhancement (b) which accompanied a SAR arc whose red-line intensity is shown in panel (d). The radar-scan data show a density trough at all heights at the latitude of the arc and a corresponding increase in electron temperature to >2500°K at the *F* region peak height near 480 km. Panel (c) superimposes convection velocity measurements made with the DMSP drift meter (solid line) and with the Millstone Hill radar (discrete points). The close relationship between the location of the SAR arc, the trough, and the isolated, more equatorward, region of westward convection was observed throughout the event (from Foster *et al.*, 1994).

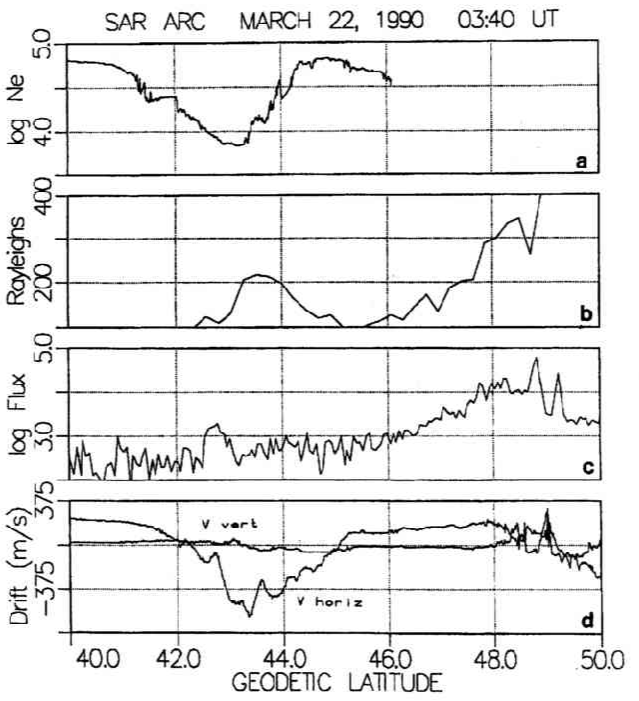

Fig. 9. Composite of the magnetospheric and ionospheric features associated with a SAR arc. See text for details of the data presented. Sunward convection was associated with the arc throughout the event (from Foster *et al.*, 1994).

A region of low-energy ion precipitation (<800 eV) was observed immediately equatorward of the SAR arc (panel 9(c)) and appears to mark the equatorward extent of the magnetospheric ion population. The equatorward limit of the plasmasheet electrons (not shown) coincided with the extent of the bright aurora (46° latitude in Fig. 9). Anderson *et al.* (1991) found that all SAID events observed at MLT < 22 hours occurred in the equatorward portion of such a double-peaked sunward convection pattern. Our observation that the CPS electrons extended equatorward to the poleward edge of the SAID convection and SAR arc, while an ion precipitation feature was located at its equatorward edge, is also consistent with a separation of the ion and electron equatorward penetration boundaries and with the mechanism proposed by Southwood and Wolf (1978).

3. Summary

Incoherent scatter radar observations provide a powerful technique for investigating magnetosphere-ionosphere coupling phenomena. Continuous observations made near the low-latitude footprint of significant magnetospheric boundaries and features permit the temporal evolution, frequency of occurrence, and spatial characteristics of the ionospheric phenomena to be determined. Combination of the radar data with ground-based optical observations or satellite overflights provides a rich data resource for the interpretation of important geophysical phenomena.

The sub-auroral and mid-latitude boundary region phenomena studied from Millstone Hill provide an example of the types of investigations which can be made from such facilities. The very important auroral/polar cap boundary is the location of the EISCAT/Svalbard radar and many significant contributions to the study of very-high-latitude magnetosphere-ionosphere coupling phenomena can be expected to the result from this new facility.

This report has been prepared with the support of Nagoya University while the author held an appointment as Visiting Professor at the Solar Terrestrial Environment Laboratory, Nagoya University. The incoherent scatter radar research program at Millstone Hill is supported by a Cooperative Agreement between the U.S. National Science Foundation and the Massachusetts Institute of Technology. The participation of the staff of the Atmospheric Sciences Group of the MIT Haystack Observatory in the work reported here is gratefully acknowledged.

REFERENCES

Anderson, P. C., R. A. Heelis, and W. B. Hanson, The ionospheric signatures of rapid subauroral drifts, *J. Geophys. Res.*, **96**, 5785–5792, 1991.

Buchau, J., E. J. Weber, D. N. Anderson, H. C. Carlson, Jr., J. G. Moore, B. W. Reinisch, and R. C. Livingston, Ionospheric structures in the polar cap: Their origin and relationship to 250-MHz scintillations, *Radio Sci.*, **20**, 325–328, 1985.

Foster, J. C., Storm-time plasma transport at middle and high latitudes, *J. Geophys. Res.*, **98**, 1675–1689, 1993.

Foster, J. C., C. del Pozo, K. Groves, and J.-P. St.-Maurice, Radar observations of the onset of current-driven instabilities in the topside ionosphere, *Geophys. Res. Lett.*, **15**, 160–163, 1988.

Foster, J. C., M. J. Buonsanto, M. Mendillo, D. Nottingham, F. J. Rich, and W. Denig, Coordinated stable auroral red arc observations: Relationship to plasma convection, *J. Geophys. Res.*, **99**, 11,429–11,439, 1994.

Galperin, Y., V. N. Ponomarev, and A. G. Zosimova, Plasma convection in the polar ionosphere, *Ann. Geophys.*, **30**, 1–7, 1974.

Mendillo, M., J. Baumgardner, and J. Providakes, Coordinated optical and radio studies of ionospheric disturbances: initial results from Millstone Hill, *J. Geophys. Res.*, **94**, 5367–5381, 1989.

Schunk, R. W., P. M. Banks, and W. J. Raitt, Effects of electric fields and other processes upon the nighttime high-latitude *F* layer, *J. Geophys. Res.*, **80**, 3121, 1976.

Southwood, D. J. and R. A. Wolf, An assessment of the role of precipitation in magnetospheric convection, *J. Geophys. Res.*, **83**, 5227–5232, 1978.

Spiro, R. W., R. A. Heelis, and W. B. Hanson, Rapid subauroral ion drifts observed by Atmospheric Explorer C, *Geophys. Res. Lett.*, **6**, 657–660, 1979.

St.-Maurice, J.-P. and W. B. Hanson, Ion frictional heating at high latitudes and its possible use for an in situ determination of neutral thermospheric winds and temperatures, *J. Geophys. Res.*, **87**, 7580, 1982.

Yeh, H.-C. and J. C. Foster, Storm-time heavy ion outflow at mid-latitude, *J. Geophys. Res.*, **95**, 7881–7891, 1990.

Yeh, H.-C., J. C. Foster, F. J. Rich, and W. Swider, Storm-time electric field penetration observed at mid-latitude, *J. Geophys. Res.*, **96**, 5707–5721, 1991.